Published in final edited form as:
*J Microsc*. 2012 January ; 245(1): 34–42. doi:10.1111/j.1365-2818.2011.03541.x.

# Limitations of Using Micro Computed Tomography to Predict Bone-Implant Contact and Mechanical Fixation

**Shuo Liu**, **Joseph Broucek**, **Amarjit S. Virdi**, and **D. Rick Sumner***
Department of Anatomy and Cell Biology, Rush University Medical Center, Chicago, IL, USA

## Abstract

Fixation of metallic implants to bone through osseointegration is important in orthopedics and dentistry. Model systems for studying this phenomenon would benefit from a non-destructive imaging modality so that mechanical and morphological endpoints can more readily be examined in the same specimens. The purpose of this study was to assess the utility of an automated micro computed tomography (μCT) program for predicting bone-implant contact (BIC) and mechanical fixation strength in a rat model. Femurs in which 1.5 mm diameter titanium implants had been in place for four weeks were either embedded in polymethylmethacrylate (PMMA) for preparation of 1 mm thick cross-sectional slabs (16 femurs: 32 slabs) or were used for mechanical implant pull-out testing (n = 18 femurs). All samples were scanned by μCT at 70 kVp with 16 μm voxels and assessed by the manufacturer's software for assessing “osseointegration volume per total volume” (OV/TV). OV/TV measures bone volume per total volume (BV/TV) in a 3-voxel thick ring that by default excludes the 3 voxels immediately adjacent to the implant in order to avoid metal-induced artifacts. The plastic-embedded samples were also analyzed by backscatter scanning electron microscopy (bSEM) to provide a direct comparison of OV/TV with a well-accepted technique for BIC. In μCT images in which the implant was directly embedded within PMMA, there was a zone of elevated attenuation (> 50% of the attenuation value used to segment bone from marrow) which extended 48 μm away from the implant surface. Comparison of the bSEM and μCT images showed high correlations for BV/TV measurements in areas not affected by metal-induced artifacts. In addition for bSEM images, we found that there were high correlations between peri-implant BV/TV within 12 μm of the implant surface and BIC (correlation coefficients ≥ 0.8, $p < 0.05$). OV/TV as measured on μCT images was not significantly correlated with BIC as measured on the corresponding bSEM images. However, OV/TV was significantly, but weakly, correlated with implant pull-out strength ($r=0.401$, $p=0.049$) and energy to failure ($r=0.435$, $p=0.035$). Thus, the need for the 48 μm thick exclusion zone in the OV/TV program to avoid metal-induced artifacts with the scanner used in this study means that it is not possible to make bone measurements sufficiently close to the implant surface to obtain an accurate assessment of BIC. Current generation laboratory-based μCT scanners typically have voxel sizes of 6–8 μm or larger which will still not overcome this limitation. Thus, peri-implant bone measurements at these resolutions should only be used as a guide to predict implant fixation and should not be over-interpreted as a measurement of BIC. Newer generation laboratory-based μCT scanners have several improvements including better spatial resolution and x-ray sources and appear to have less severe metal-induced artifacts, but will need appropriate validation as they become available to researchers. Regardless of the μCT scanner being used, we recommend that detailed validation studies be performed for any study using metal implants since variation in the composition and geometry of the particular implants used may lead to different artifact patterns.

*Correspondence to D. Rick Sumner, Department of Anatomy and Cell Biology, Rush University Medical Center, 600 South Paulina Street, Rm 507, Chicago, IL, 60612, Tel: 312-912-5511, Fax: 312-942-5744, rick_sumner@rush.edu.

**Keywords**

μCT; osseointegration; implant fixation; metal-induced artifact; bSEM

## INTRODUCTION

Osseointegration is an important factor in determining the clinical outcome of implant fixation (Albrektsson, Branemark, Hansson, and Lindstrom, 1981). Branemark et al. first introduced the concept of osseointegration to describe direct bone-implant contact (BIC) at the level of light microscopy (Branemark, 1959;Branemark, 1983). Since Branemark's initial introduction, osseointegration has been studied intensively using histological techniques (Sumner, Jasty, Jacobs, Urban, Bragdon, Harris, and Galante, 1993;Stadlinger et al., 2007;Brånemark, 1996;Albrektsson, Branemark, Hansson, and Lindstrom, 1981). Backscatter scanning electron microscopy (bSEM) has also been used to conduct detailed observations of BIC (Sovak, Weiss, and Gotman, 2000;Albrektsson, Branemark, Hansson, and Lindstrom, 1981;Lin, Xu, Zhang, and de Groot, 1998;Svehla, Morberg, Zicat, Bruce, Sonnabend, and Walsh, 2000). The evaluation of both histological and bSEM images requires intensive work in terms of specimen preparation. In addition, the results of both evaluations can be influenced by technical errors due to specimen damage during preparation, and using histology or bSEM limits the ability to correlate the findings with mechanical measurements of implant fixation. Therefore, a convenient and reliable technique to measure BIC (osseointegration) through non-destructive means would be useful.

Micro computed tomography (μCT) is an efficient, non-destructive, and reproducible 3-D imaging technique that analyzes bone architecture and density under various conditions without sophisticated specimen preparation (Bagi, Hanson, Andresen, Pero, Lariviere, Turner, and Laib, 2006;Cartmell, Huynh, Lin, Nagaraja, and Guldberg, 2004;Kapadia et al., 1998;Ruegsegger, Koller, and Muller, 1996;Ding, Odgaard, and Hvid, 1999). μCT has also been applied to analyze peri-implant bone volume (De Ranieri, Virdi, Kuroda, Shott, Leven, Hallab, and Sumner, 2005;De Ranieri, Virdi, Kuroda, Healy, and Sumner, 2005;Kuroda, Virdi, Li, Healy, and Sumner, 2004). Some investigators have reported methods to quantify BIC with μCT (Butz, Ogawa, Chang, and Nishimura, 2006;Xing, Hasty, and Smith, 2006;Gabet, Kohavi, Voide, Mueller, Muller, and Bab, 2010). These studies suggest that bone-implant contact could be another application for μCT, although one of these studies has reported lack of correlation between μCT and histology for regions within 24 μm of the implant surface (Butz, Ogawa, Chang, and Nishimura, 2006). Recently, a new μCT program was developed to quantify BIC, with the output variable called osseointegration volume/total volume (OV/TV), and this algorithm has been applied in at least one animal model (Gao, Luo, Hu, Xue, Zhu, and Li, 2009). According to the default setup of the program, OV/TV calculates BV/TV in a three voxel thick ROI that excludes the 3 voxels closest to the implant surface in order to avoid metal-induced artifacts. Although this μCT program has the advantage of being automated and requires no special specimen preparation, μCT evaluation has limited ability to measure bone adjacent to the implant surface. (Butz, Ogawa, Chang, and Nishimura, 2006). Therefore, the primary goal of the current study was to evaluate the accuracy of μCT-based OV/TV as a means of quantifying BIC in a rat model of femoral intramedullary implantation. We also examined the relationship between OV/TV and mechanical fixation strength.

# METHODS AND MATERIALS

## Study design

The study started by assessing metal-induced artifacts using a cylindrical titanium implant embedded in polymethylmethacrylate (PMMA), in the absence of bone, followed by examination of two group of specimen (Fig. 1). The first group had sixteen 1 mm thick PMMA embedded slabs from 16 rats in which a titanium implant had been surgically placed for a period of 4 weeks. μCT-based OV/TV measurement was compared to bSEM-based BIC in these PMMA embedded samples. The second group had whole femurs from 18 rats in which the titanium implant had been in place for 4 weeks. μCT-based OV/TV measurements were compared to mechanical fixation in these samples. Another 16 PMMA embedded samples were examined by bSEM to test the fundamental assumption of the μCT-based OV/TV measurement that the presence of bone somewhat removed from the implant surface reflects BIC.

## Preparation of samples

Samples from previously approved IACUC studies were included in this study. Male Sprague-Dawley rats (400–425g, Harlan, IN, USA) received unilateral intramedullary implantation of solid commercially pure titanium cylinders (1.5 mm diameter, 20 mm long) into the distal femur. Both femurs were harvested four weeks after surgery. 16 femurs were fixed in 10% formalin for 24 hours, dehydrated and embedded in PMMA. The PMMA-embedded femurs were sectioned perpendicular to the long axis of the implant into 1mm thick slabs (Isomet 5000, Buehler, Lake Bluff, IL, US) and 32 slabs were included in this study. The whole femurs were from 18 animals and the bones were wrapped with saline-soaked gauze and stored at −20°C for μCT scanning and mechanical testing. In addition, one of the titanium implants was embedded directly in PMMA (i.e., embedded in the absence of bone) and sectioned perpendicular to the long axis of the implant into a 1mm thick slab to test for metal-induced artifacts in the μCT images.

## μCT

All PMMA slabs as well as the whole femurs were scanned perpendicular to the long axis of the implant by μCT (Scanco 40, Wayne, PA, US) at 70 kVp, 144 μA, 300-ms integration time, 500 projections per 180°, using a cone-beam architecture in which the cone-beam angle is less than 1°. X-ray filtering occurred with 0.5 mm aluminum (and a 0.13 mm beryllium window built into the x-ray tube). The CCD array was 1024 by 256 pixels, with a pixel pitch 24 μm, coupled to a CsI scintiallator. The 10% MTF for this scanner is approximately 1.4 voxels (~22 μm with 16 μm voxels and ~11 μm with 8 μm voxels). The voxels are isotropic. All specimens were scanned using 16 μm voxels, while the PMMA slab with implant only was also scanned using 8 μm voxels. The scanning medium for the embedded specimens was the PMMA and the medium for the whole femurs was saline. Images were processed by a bone Gaussian filter σ=1.5 support=2 and a titanium Gaussian filter σ=2 support=2 for reconstruction. The image grayscale values are reported in terms of mg hydroxyapatite per cubic centimeter (mg HA/ccm), using the scanner software to make the conversion from attenuation values to a standardized unit. OV/TV for each slice was analyzed by the manufacturer's software using bone segmentation and titanium segmentation thresholds of 829 mg HA/ccm and 2517 HA/ccm, respectively. These threshold values were chosen because they provided the most accurate measurements of BV/TV in the ROI assessed by the OV/TV program and of the implant area, respectively (see on-line Supplementary Material). OV/TV was defined as BV/TV in a ROI including the $4^{th}$, $5^{th}$ and $6^{th}$ voxels away from the implant surface, which was 48 μm to 96 μm from the implant surface with a voxel size of 16 μm, thereby eliminating the 3 voxels closest to the implant (Fig. 2). In 18 whole femurs, 5 sites which were evenly distributed along the length of the

implant were scanned. Each site included 100 slices oriented perpendicular to the long axis of the implant and bone. OV/TV was calculated based on all 5 sites. Thus, we sampled approximately 8 mm (500 slices) of the implant and surrounding bone, representing 40% of the length of the implant.

### bSEM Imaging

After μCT scanning, the PMMA slabs were ground to a thickness of approximately 0.5 mm with a series of grinding papers, ending with 3 μm polishing paper (Phoenix 400, Buehler, Lake Bluff, IL, US). The thickness before and after grinding was carefully measured by caliper. The polished slabs were coated with a layer of carbon to enable the conduction of the electron beam (Cressington carbon coater model 108). bSEM images were taken at 25kV, a beam current of 100μA, a working distance of 15mm, and a magnification of 90X (Hitachi 3000N, Pleasanton, CA) perpendicular to the long axis of the implant. bSEM-based BIC was analyzed by using a line-intersect method on digital images with 2.2 μm pixel size. Briefly, 48 evenly distributed test lines originating from the center of the implant were evaluated as positive or negative for bone at the intersection between each test line and the surface of the implant. BIC was defined as the number of bone positive intersections divided by 48. BIC from line-intersect method with 48 lines was highly correlated with BIC from line-intersect method with either 72 lines or 96 lines.

On the bSEM images of the 16 PMMA slabs, BV/TV in 10 consecutive concentric 1 pixel thick ROIs starting from the implant surface (Fig. 3) was measured (Image J, NIH, Bethesda, MD) and correlated with bSEM-based BIC determined on the same specimens. The bSEM images were carefully matched with the corresponding μCT images (Fig. 4). Briefly, after μCT scanning, the samples were ground to remove a certain thickness so that a surface could be prepared for bSEM. The height of this thickness divided by the slice thickness of the μCT images yields the number of slices, counted from the first μCT slice to the slice matching the bSEM image. For example, if the ground down thickness is 800 μm and the voxel size is 16 μm, then the 50th μCT slice down from the first μCT slice should match the bSEM image. This was verified by inspection of morphological features on the contiguous μCT slices and the bSEM image. The OV/TV value on the corresponding μCT image was correlated with the bSEM-based BIC.

### Mechanical pull-out testing

In the whole femur group, the strength of implant fixation with the host bone was measured by a mechanical pull-out test as described in detail elsewhere (Kuroda, Virdi, Li, Healy, and Sumner, 2004). To prepare the specimens, all but the distal 5 mm of the femur was encased in dental acrylic (Lang Dental, Wheeling, IL, US). The bone surrounding the distal-most aspect of the implant was carefully removed to expose the distal 3–4 mm of the implant. The exposed implant was then gripped, and S hooks were placed at either end of the specimen to permit coaxial alignment of the implant in the direction of force. Pull-out testing was conducted at a displacement rate of 0.25 mm/min to failure with the force recorded in Newtons (Instron, Canton, MA, US). Pull-out strength ($N/mm^2$) was calculated by dividing the force (N) at the point of failure by the nominal surface area of the implant in contact with tissue ($mm^2$). This contact area was calculated as the total nominal surface area of the rod (based on the implant length and circumference) minus the area of the implant used for gripping. The pull-out energy to failure (N-mm) was also calculated. The strength of implant fixation, energy to failure and stiffness were correlated with μCT OV/TV.

### Metal-induced artifact analysis

The metal-induced artifact was evaluated on one μCT image of the implant embedded directly in PMMA. The μCT scanning setting is described above in the μCT section. The

average attenuation per voxel in concentric 1-voxel thick ROIs surrounding the implant was determined using images collected with both 8 μm and 16 μm voxels (Image J, NIH, Bethesda, MD). As a control, the attenuation value of PMMA was determined for a concentric 1 voxel thick ROI, which was 1mm away from the implant surface. This average control value was subtracted from the attenuation values of the ROIs located closer to the implant. Because there was no bone present in this sample, any value above 0 indicates the magnitude of the error induced by the presence of the implant.

### Statistics

SPSS for Windows (Version 15) was used for data management and statistical analysis. Pearson correlations were obtained to investigate relationships between the variables. BV/TV in each consecutive concentric ROI was correlated with bSEM-based BIC (n=16). μCT OV/TV was correlated with bSEM-based BIC from the corresponding images (n=16). The pull-out strength, energy to failure and stiffness were correlated with OV/TV (n=18). A significance level of p=0.05 was used for all statistical tests.

## RESULTS

### Metal-induced artifact

For the sample containing only the titanium implant embedded directly in PMMA, the attenuation values in the μCT image within the first 20 to 30 μm of the implant surface were higher than the chosen bone segmentation value (Fig. 5). The grayscale values from PMMA using both 8 μm and 16 μm resolutions were around 15 mg HA/ccm.

### Predicting BIC as a function of distance from implant surface

The correlation coefficients between bSEM-based BV/TV for ROIs located within 18 μm of the implant surface and bSEM-based BIC were significant ($p<0.05$, Fig. 6). The correlation coefficients were greater than 0.8 for ROIs within 12 μm of the implant surface. However, for ROIs farther than 18 μm from the implant surface, the correlations were not significant (Fig. 6).

### Accuracy of μCT in the prediction of BIC

OV/TV was not significantly correlated with bSEM-based BIC ($r = 0.074$, $p > 0.05$). Some of the corresponding images from bSEM and μCT had a similar appearing bone-implant interface (Figs. 7A, 7B). However, other samples had small gaps (< 10 μm) between the bone and the implant surface that were apparent on the bSEM image, but not discernable on the μCT image (Figs. 7C, 7D). In addition, some samples had a very thin layer of peri-implant bone (< 20 μm thick), with or without apparent contact with the implant (Figs. 8A, B). Since the OV/TV program eliminates the first 48 μm (when scanning at 16 μm resolution) or 24 μm (when scanning at 8 μm resolution), it is possible for samples similar to those shown in Fig. 7 to have similar OV/TV values when the bSEM-based BIC values are very different.

### Accuracy of μCT in the prediction mechanical fixation

The strength ($r=0.401$, $p=0.049$, Fig. 9A) and energy to failure ($r=0.435$, $p=0.035$, Fig. 9B) were significantly correlated with μCT OV/TV, although stiffness was not significantly correlated with μCT OV/TV ($r=0.278$, $p=0.130$).

## DISCUSSION

In this study, we demonstrated that the μCT-based assessment of OV/TV lacked significant correlation with bSEM-based bone-implant contact, but had a significant correlation with the mechanical fixation of implants. The work presented here shows that accurate estimates of BIC using μCT will require unbiased assessment of bone within 12 μm of the implant surface. Thus, the metal-induced artifact zone which was found to extend 32 μm outward from the implant when using 16 μm voxels needs to be significantly reduced. Improved spatial resolution of μCT scans would also be helpful.

Other authors have reported on metal-induced artifacts. One study using a similar rat model with smaller titanium implants demonstrated that metal-induced artifacts in μCT images were significant within the first 24 μm from of the implant surface (Butz, Ogawa, Chang, and Nishimura, 2006). Another study using a sheep model and larger implants suggested that the metal-induced artifact region extends 60 μm from the implant interface (Stoppie, van der Waerden, Jansen, Duyck, Wevers, and Naert, 2005). Therefore, characterizing the artifact zone around metal implants is a key factor in using μCT to evaluate BIC. Because of partial volume effects on the order of 1 to 2 voxels (10% MTF is about 1.4 voxels) and scatter effects, preliminary studies were performed and indicated that eliminating the 3 voxels closest to the detected surface was necessary to enable segmentation of bone from marrow. We recommend that researchers perform similar studies with their scanner and implants before interpreting results from manual or automated evaluations of bone in close proximity to metal implants because the artifact area is likely to be specific to the scanning conditions used.

The OV/TV program makes the assumption that if bone is present in the region of interest (i.e., in the region from 48 to 96 μm from the implant surface in the present study, where 16 μm voxels were used), then it is likely that bone is also in contact with the implant surface. We tested this assumption using bSEM and found that only measurements of BV/TV within 18 μm of the implant interface were correlated with the actual BIC, with the measurements within 12 μm strongly correlated ($r > 0.8$). It follows that the assessment of OV/TV as performed in the present study did not occur in a region where bone volume is known to be highly correlated with BIC. The bSEM findings indicate that if metal-induced artifacts can be significantly reduced adjacent to the implant surface, then it should be possible for the OV/TV algorithm to provide accurate BIC estimates. Specifically, with the current OV/TV algorithm which measures bone in voxels 4–6 from the implant surface, the voxel size would need to be reduced to approximately 1–2 μm to obtain an accurate assessment of BIC. Another strategy would be to reduce the size of the unmeasured zone to 2 voxels from 3 voxels and to restrict the OV/TV measurement to a one voxel thick ROI. In this situation, assuming a minimized metal-induced artifact zone, the needed resolution would be on the order of 3 μm voxels. This is possible with the newer generation μCT scanners. These new scanners not only offer better resolution, but also have better x-ray sources and tomography capabilities, which will lessen metal-induced artifacts around implants.

Some of the corresponding μCT and bSEM images highlight the need for improved spatial resolution. In particular, cases where there were very small bone-implant interface gaps and cases where the peri-implant bone was very thin indicate the need for improved resolution. For instance, the bSEM images showed that the peri-implant bone was sometimes less than 20 μm thick and could be separated from the implant surface by very small gaps (often less than 10 μm). Thus, it is perhaps not surprising that we found cases of low bSEM-based BIC in which the corresponding OV/TV from μCT was high. The combination of relatively large voxel sizes and the need to eliminate the first few voxels from the analysis means that the automated program misses very thin trabeculae contacting or in close proximity to the

implant. Thus, the bSEM data indicate that near surface bone morphometry may or may not be reflective of the actual BIC. The implication is that even if the metal-induced artifact could be reduced it will also be important to have better resolution than is currently available in the most commonly used laboratory μCT scanners.

Although the default setup of the automated μCT OV/TV program successfully excludes most of the metal-induced artifact and secures an accurate assessment of BV/TV in the region analyzed, the eliminated distance itself is too large to allow an accurate prediction of BIC. A possible solution for this problem is to subtract the metal-induced artifact from the original images of the implantation specimens by scanning a reference implant in the same medium (Gabet, Kohavi, Voide, Mueller, Muller, and Bab, 2010). Then, the eliminated distance in the μCT OV/TV program might be unnecessary. The limitations imposed by relatively large voxel sizes compared to the morphology of the bone being interrogated would not be solved with this approach.

Although the automated measurement of OV/TV currently has a limited ability to reflect bone-implant contact, the present study indicates that it is already a useful technique to predict the mechanical fixation of implants with the host bone. Specifically, bone volume in the region close to implant surface (i.e., the OV/TV measurement) can predict mechanical fixation of the implant. Other studies have examined the correlation between mechanical fixation and μCT measured BV/TV in ROIs within 200 μm (Tami, Leitner, Baucke, Mueller, van Lenthe, Muller, and Ito, 2009) and 500 μm (Schouten, Meijer, van den Beucken, Spauwen, and Jansen, 2009) of the implant interface, and reported poor correlations. It is also important to realize that the mechanical fixation of the implant is not only related to the bone close to the implant interface and in direct contact with the implant, but also is critically dependent on structural characteristics of peri-implant bone trabeculae in a relatively broad zone around the implant (Gabet, Kohavi, Voide, Mueller, Muller, and Bab, 2010). In some samples of this study, we detected some bone on the pulled out implant, which indicates that failure happened on the peri-implant bone trabeculae in these samples. So, peri-implant bone trabeculae in these samples may account for the mechanical fixation more than BIC, which may also explain the poor correlation between OV/TV and mechanical test in this study.

This study was not designed to investigate the effects of time, implant composition or shape on the ability of μCT to estimate BIC or implant fixation. We would like to note that even though the samples were all from one time point post surgery (4 weeks), there was a very wide range in BIC (essentially 0% to 90%), meaning that the data set was suitable for examining the relationship between μCT-based and bSEM-based parameters and between OV/TV and mechanical fixation. The approach presented here can serve as a model for future investigations in which researchers plan to interrogate implants of different composition or shape with μCT.

It is important to perform studies similar to the present one because implants with different surface roughness, other surface modifications or using other materials such as cobalt-based alloys may have different results. Several manufacturers have recently introduced higher resolution laboratory scanners, and initial scans with this new equipment suggest that it may be possible to improve upon non-destructive assessments of the bone-implant interface (unpublished data). In order to use the μCT OV/TV program or even manual determination of bone-implant contact with confidence we recommend that researchers assess the utility of the measurement for their specific study conditions. The present paper provides a useful approach to these sorts of validation studies. We conclude that the μCT OV/TV data collected at the resolution used in the present study should only be considered as a guide to predict implant fixation and should not be over-interpreted as a measurement of BIC.

## Supplementary Material

Refer to Web version on PubMed Central for supplementary material.

## Acknowledgments

Andres Laib discussed the project with the authors and made helpful suggestions. The study was funded by NIH grant AR054171 and was conducted with the help of the microCT Core Facility at Rush University Medical Center with special help from Naomi Kotwal and Dana Glock.

## Literature Cited

Albrektsson T, Branemark PI, Hansson HA, Lindstrom J. Osseointegrated titanium implants. Requirements for ensuring a long-lasting, direct bone-to-implant anchorage in man. Acta Orthopaedica Scandinavica. 1981; 52:155–170. [PubMed: 7246093]

Bagi CM, Hanson N, Andresen C, Pero R, Lariviere R, Turner CH, Laib A. The use of micro-CT to evaluate cortical bone geometry and strength in nude rats: correlation with mechanical testing, pQCT and DXA. Bone. 2006; 38:136–144. [PubMed: 16301011]

Branemark PI. Vital microscopy of bone marrow in rabbit. Scandinavian Journal of Clinical Laboratory Investigation. 1959; 11:1–82. [PubMed: 13658913]

Branemark PI. Osseointegration and its experimental background. Journal of Prosthetic Dentistry. 1983; 50:399–410. [PubMed: 6352924]

Brånemark, R. A biomechanical study of osseointegration: in-vivo measurements in rat, rabbit, dog and man. Göteborg: 1996.

Butz F, Ogawa T, Chang TL, Nishimura I. Three-dimensional bone-implant integration profiling using micro-computed tomography. Int J Oral Maxillofac Implants. 2006; 21:687–695. [PubMed: 17066629]

Cartmell S, Huynh K, Lin A, Nagaraja S, Guldberg R. Quantitative microcomputed tomography analysis of mineralization within three-dimensional scaffolds in vitro. J Biomed Mater Res. 2004; 69A:97–104.

De Ranieri A, Virdi AS, Kuroda S, Healy KE, Sumner DR. Saline irrigation does not affect bone formation or implant fixation strength in a rat model. Journal of Biomedical Materials Research Part B: Applied Biomaterials. 2005; 74B:712–717.

De Ranieri A, Virdi AS, Kuroda S, Shott S, Leven RM, Hallab NJ, Sumner DR. Local application of rhTGF-β2 enhances peri-implant bone volume and bone-implant contact in a rat model. Bone. 2005; 37:55–62. [PubMed: 15869922]

Ding M, Odgaard A, Hvid I. Accuracy of cancellous bone volume fraction measured by micro-CT scanning. Journal of Biomechanics. 1999; 32:323–326. [PubMed: 10093033]

Gabet Y, Kohavi D, Voide R, Mueller TL, Muller R, Bab I. Endosseous implant anchorage is critically dependent on mechanostructural determinants of peri-implant bone trabeculae. J Bone Miner Res. 2010; 25:575–583. [PubMed: 19653813]

Gao Y, Luo E, Hu J, Xue J, Zhu S, Li J. Effect of combined local treatment with zoledronic acid and basic fibroblast growth factor on implant fixation in ovariectomized rats. Bone. 2009; 44:225–232. [PubMed: 19056525]

Kapadia RD, et al. Applications of micro-CT and MR microscopy to study pre-clinical models of osteoporosis and osteoarthritis. Technol Health Care. 1998; 6:361–372. [PubMed: 10100939]

Kuroda S, Virdi AS, Li P, Healy KE, Sumner DR. A low temperature biomimetic calcium phosphate surface enhances early implant fixation in a rat model. Journal of Biomedical Materials Research. 2004; 70A:66–73. [PubMed: 15174110]

Lin H, Xu H, Zhang X, de Groot K. Tensile tests of interface between bone and plasma-sprayed HA coating-titanium implant. J Biomed Mater Res. 1998; 43:113–122. [PubMed: 9619429]

Ruegsegger P, Koller B, Muller R. A microtomographic system for the nondestructive evaluation of bone architecture. Calcified Tissue International. 1996; 58:24–29. [PubMed: 8825235]

Schouten C, Meijer GJ, van den Beucken JJ, Spauwen PH, Jansen JA. The quantitative assessment of peri-implant bone responses using histomorphometry and micro-computed tomography. Biomaterials. 2009; 30:4539–4549. [PubMed: 19500840]

Sovak G, Weiss A, Gotman I. Osseointegration of Ti6Al4V alloy implants coated with titanium nitride by a new method. Journal of Bone and Joint Surgery. 2000; 82:290–296. [PubMed: 10755443]

Stadlinger B, et al. Influence of extracellular matrix coatings on implant stability and osseointegration: An animal study. J Biomed Mater Res B Appl Biomater. 2007; 83:222–231. [PubMed: 17318830]

Stoppie N, van der Waerden JP, Jansen JA, Duyck J, Wevers M, Naert IE. Validation of microfocus computed tomography in the evaluation of bone implant specimens. Clin Implant Dent Relat Res. 2005; 7:87–94. [PubMed: 15996355]

Sumner DR, Jasty M, Jacobs JJ, Urban RM, Bragdon CR, Harris WH, Galante JO. Histology of porous-coated acetabular components: 25 cementless cups retrieved after arthroplasty. Acta Orthopaedica Scandinavica. 1993; 64:619–626. [PubMed: 8291405]

Svehla M, Morberg P, Zicat B, Bruce W, Sonnabend D, Walsh WR. Morphometric and mechanical evaluation of titanium implant integration: comparison of five surface structures. Journal of Biomedical Materials Research. 2000; 51:15–22. [PubMed: 10813740]

Tami AE, Leitner MM, Baucke MG, Mueller TL, van Lenthe GH, Muller R, Ito K. Hydroxyapatite particles maintain peri-implant bone mantle during osseointegration in osteoporotic bone. Bone. 2009; 45:1117–1124. [PubMed: 19679208]

Xing Z, Hasty KA, Smith RA. Administration of pamidronate alters bone-titanium attachment in the presence of endotoxin-coated polyethylene particles. J Biomed Mater Res B Appl Biomater. 2006; 83:354–358. [PubMed: 17385218]

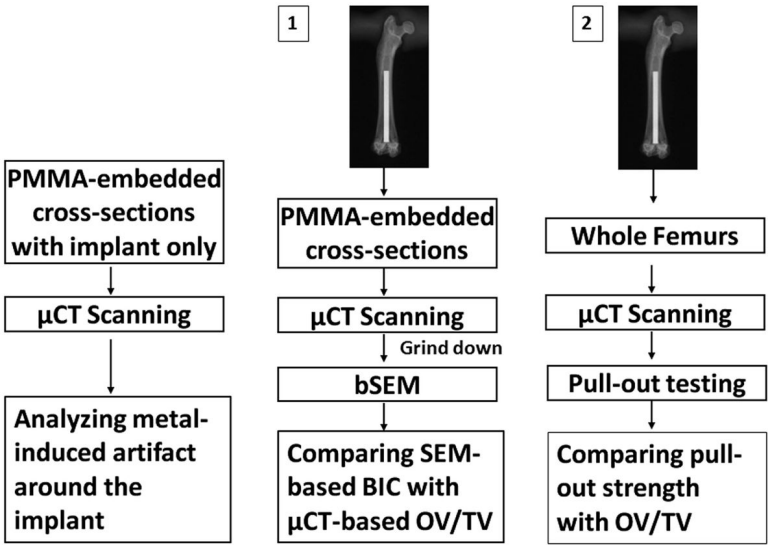


**Figure 1.**

Study design. One PMMA-embedded slab with implant only was used to analyze metal-induced artifacts. Sixteen 1 mm thick PMMA-embedded slabs in set 1 were scanned by μCT, and then ground down for bSEM imaging to compare SEM-based BIC with μCT-based OV/TV. Eighteen whole femurs in set 2 were scanned by μCT, and then used for mechanical pull-out testing to compare fixation strength with μCT OV/TV.

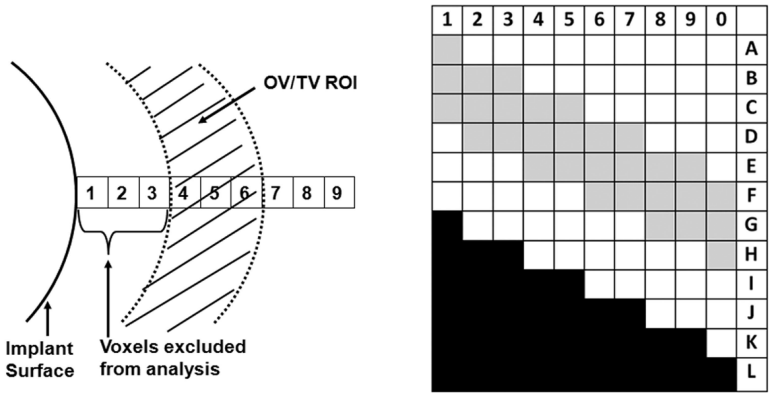


**Figure 2.**

OV/TV algorithm. On the left diagram, the black solid line represents the surface of the titanium implant. The two broken lines show the inner and outer boundaries of the ROI used for μCT OV/TV measurement (hatched area). OV/TV measures BV/TV in voxels 4, 5 and 6, eliminating the 3 voxels closest to the implant surface. On the right diagram, the grids represent the μCT voxels, with the black squares representing the implant and the gray squares representing the OV/TV ROI. In this case, voxels G1, H2, H3, I4, I5, J6, J7, K8, K9 and L0 compose the implant surface. For example, voxels C1, B1 and A1 are the voxels 4, 5 and 6 away from voxel G1. For sake of clarity, the third dimension is not shown.

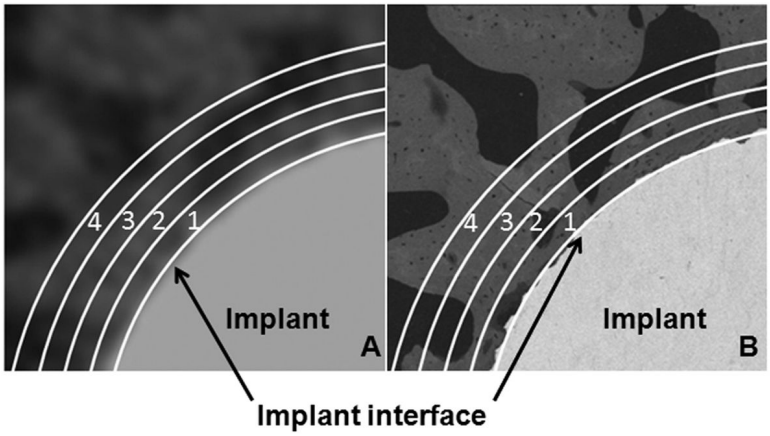


**Figure 3.**
Illustration of concentric ROIs on μCT image (A) and bSEM image (B). Part of the implant cross-section is at the lower right corner on each image. The first line close to the implant indicates the implant surface. The numbered regions represent concentric ROIs.

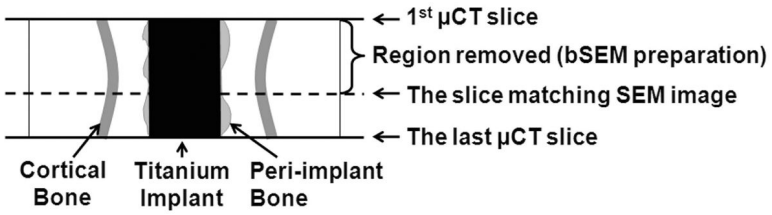


**Figure 4.**

Illustration of how bSEM images were matched with the corresponding µCT images. The physical distance between the upper solid line (first slice scanned by µCT) and the dashed line (the surface examined by bSEM after the sample was ground and polished) was used to identify the corresponding images between the two modalities.

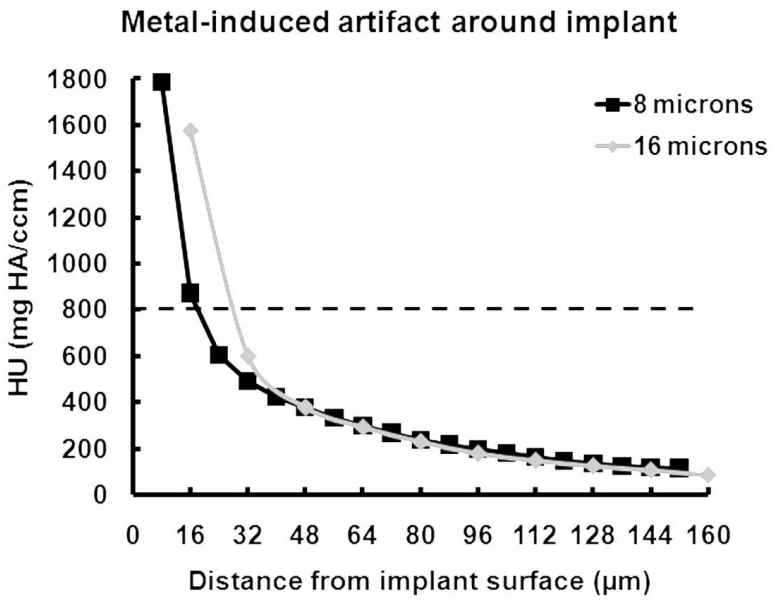


**Figure 5.**
Metal-induced artifact. The x-axis represents the distance from the implant surface and the y-axis represents the difference in attenuation value between the ROI sampled and a `control' ROI which was located 1000 μm from the implant surface. The dashed line shows the selected threshold for bone segmentation.

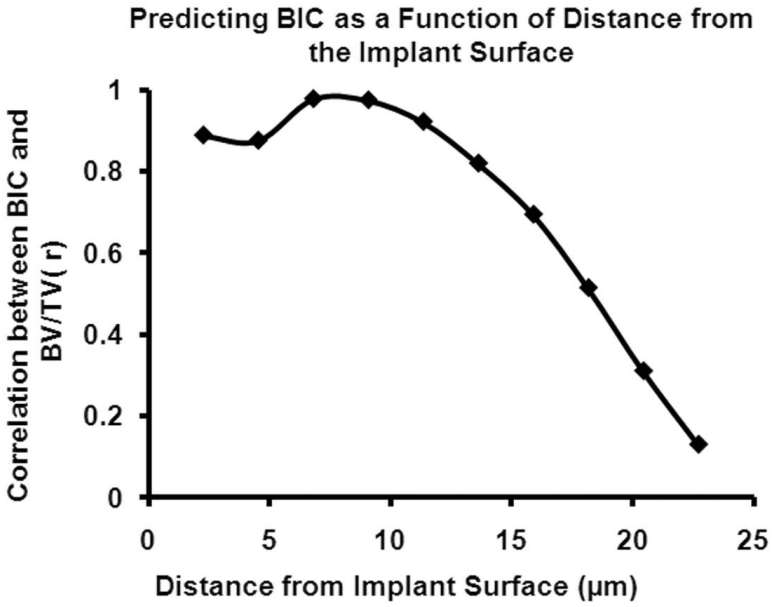


**Figure 6.**
Correlation between BV/TV in concentric ROIs at increasing distances from the implant surface and bSEM-based BIC. Note that the strength of correlation decreases to a low level and is not significant for ROIs beyond 18 μm from the implant surface.

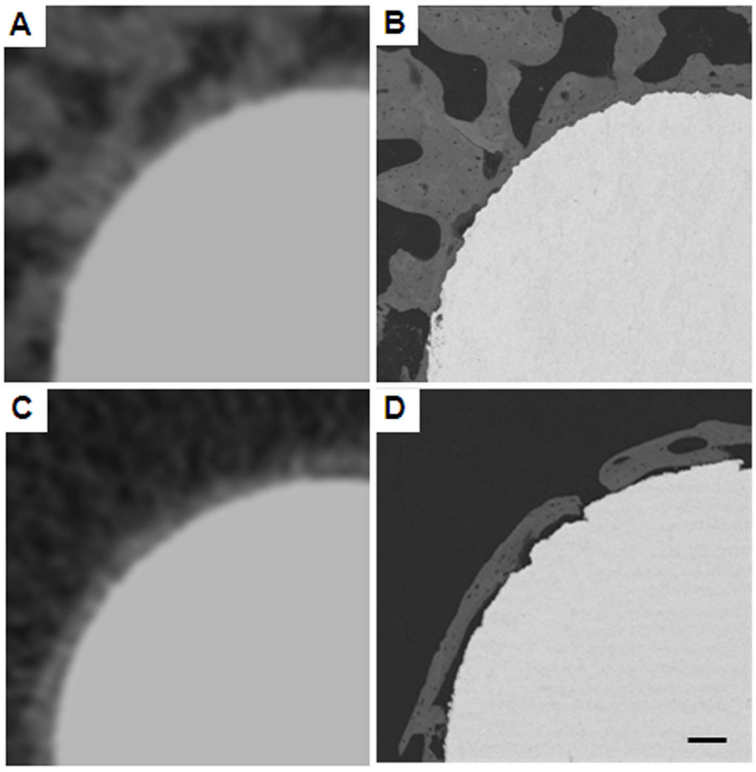


**Figure 7.**
μCT images (A, C) and corresponding bSEM images (B, D). Images A and C give a similar impression of BIC. However, images B and D show that the actual BIC can be quite different even when the μCT images seem consistent. Scale bar is 100 μm. Voxel size in the μCT images was 16 μm and the pixel size in the bSEM images was 2.2 μm.

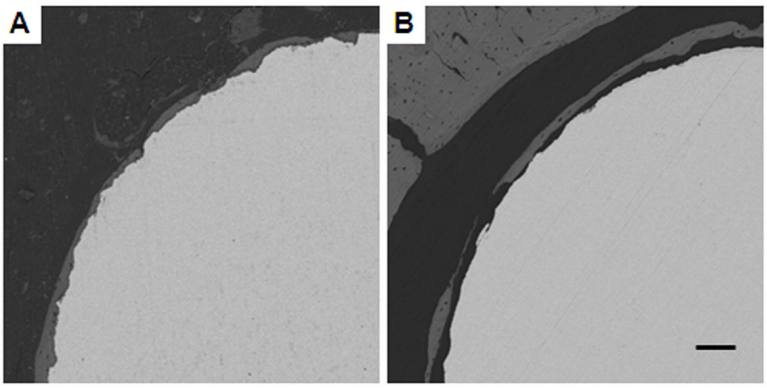


**Figure 8.**

bSEM images with a thin layer of peri-implant bone. Image A shows good BIC while Image B shows poor BIC. In both cases, there is only a thin layer of peri-implant bone and this bone occupies the region not considered by the OV/TV program (the first 48 μm away from the implant). So, although the bSEM-based BIC is different in Images A and B, their OV/TV values may be close. Scale bar is 100 μm.

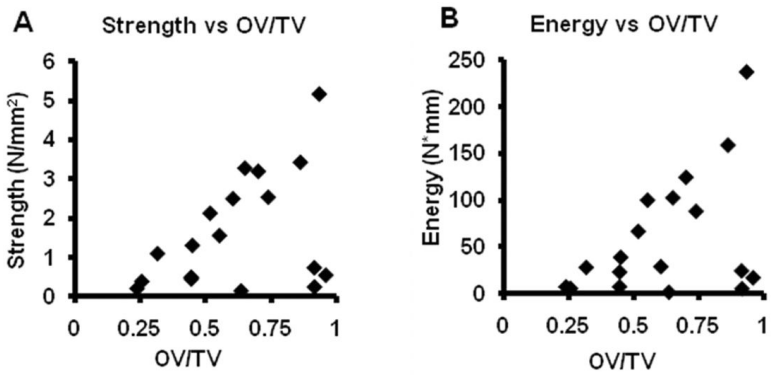


**Figure 9.**

Correlation between μCT OV/TV and mechanical testing results. Panel A shows the correlation between pull-out strength and μCT OV/TV (r=0.401, p=0.049). Panel B shows the correlation between pull-out energy to failure and μCT OV/TV (r=0.435, p=0.035).